

# RAMAN SCATTERING STUDY OF A TWO-DIMENSIONAL $S = 1$ QUANTUM SPIN SYSTEM $\text{Ni}_5(\text{TeO}_3)_4\text{Cl}_2$

A.V. PESCHANSKII, V.P. GNEZDILOV, V.I. FOMIN, V.V. EREMENKO,  
P. LEMMENS<sup>1</sup>, K.-Y. CHOI<sup>2</sup>, H. BERGER<sup>3</sup>

UDC 539.9 + 537

©2009

B. Verkin Institute for Low Temperature Physics and Engineering,  
Nat. Acad. of Sci. of Ukraine  
(47, Lenin Ave., Kharkiv 61103, Ukraine),

<sup>1</sup>Inst. Cond. Matter Physics, TU Braunschweig  
(D-38106 Braunschweig, Germany),

<sup>2</sup>Department of Physics, Chung-Ang University  
(221 Hukseok-Dong, Dongjak-Gu, Seoul 156-176, Republic of Korea),

<sup>3</sup>Ecole Polytechnique Federale  
(Lausanne CH-1015, Switzerland; e-mail: peschansky@ilt.kharkov.ua)

The transition metal tellurium oxychloride,  $\text{Ni}_5(\text{TeO}_3)_4\text{Cl}_2$ , has been investigated by the Raman scattering method at temperatures of 15–300 K. Sixty two phonon modes (of the total 69 Raman-active phonon modes allowed for the monoclinic  $C_{2h}^6$  structure) are identified in the spectra, and their behavior is analyzed. Several distinct features are observed in Raman spectra at low temperatures: (i) three low-frequency bands (22.3, 29.4, and  $49.0 \text{ cm}^{-1}$  at  $T = 15 \text{ K}$ ) with a temperature behavior characteristic of the one-magnon scattering and (ii) a band at  $56.3 \text{ cm}^{-1}$  with a pronounced temperature dependence. The origin of the low-temperature bands is discussed.

## 1. Introduction

A great deal of interest in magnetism has been recently been devoted to theoretical and experimental investiga-

tions of low-dimensional spin systems [1–3]. This interest has been stimulated by theoretical predictions of a rich phase diagram and novel magnetic properties which originate from the interplay of the geometric frustration and quantum fluctuations in low dimensions. In general, the behavior of frustrated systems is difficult to predict; the frustration can lead to a microscopic degeneracy and qualitatively to new states of matter. Magnetic systems offer good examples in the form of spin lattices, where all interactions between spins cannot be simultaneously satisfied. It is frequently assumed that the spin lattice of a magnetic system containing a transition metal is the same as the geometric arrangement of its metal ions. For complex magnetic systems, such intuitive approach is often incorrect, because the spin exchange interaction strength is not determined by the distance between two spin sites but by the overlap between their magnetic orbitals. The crystal structure, namely positions of nonmagnetic neighboring ions can affect the spin exchange interaction and hence the topology of the spin lattice.

Recently, the investigation of the ternary phase diagram  $\text{NiO-NiCl}_2\text{-TeO}_2$  has led to the synthesis of new transition-metal tellurium oxohalogenides with the general chemical formula  $\text{Ni}_5(\text{TeO}_3)_4\text{X}_2$  ( $\text{X} = \text{Br}, \text{Cl}$ ) [4]. These compounds have clearly a pronounced layered structure. The nickel ions have a  $3d^8$  electronic configuration, with spin  $S = 1$ , forming a quasi-two-dimensional magnetic structure. Each layer is made of groups of five strongly distorted Ni-octahedra into a  $[\text{Ni}_5\text{O}_{17}\text{X}_2]$  “claw unit” with some unusually short  $\text{Ni}^{2+}$ – $\text{Ni}^{2+}$  distances (Fig. 1). These units are then linked via the corner sharing to next-nearest neighbors. The magnetic properties should therefore be dictated by the

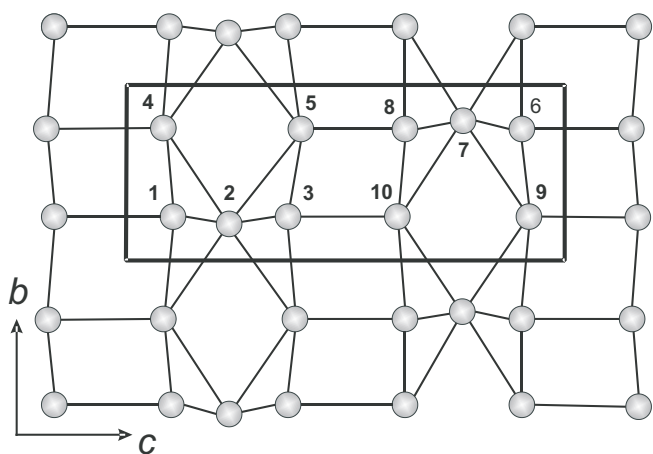


Fig. 1. Ni ion configuration in a single layer of the  $\text{Ni}_5(\text{TeO}_3)_4\text{Cl}_2$  crystal. Thick line frames Ni ions in a single unit cell

strong magnetic interaction within each “claw unit”. Because the  $\text{Ni}^{2+}$  ( $S = 1$ ) moments in a unit are arranged in an interesting double triangular topology, the frustration may play a significant role [5].

In the previous investigations, considerable efforts have been put into the basic experimental studies of  $\text{Ni}_5(\text{TeO}_3)_4\text{Cl}_2$  [4, 6, 7]. The magnetic susceptibility of  $\text{Ni}_5(\text{TeO}_3)_4\text{Cl}_2$  shows a Curie–Weiss behavior with negative Curie–Weiss temperature  $\Theta = -50$  K [4] (powder) and  $\Theta = -49$  K [7] and  $\Theta = -60$  K [8] (single crystals). The negative sign of the Curie–Weiss temperature indicates antiferromagnetic correlations between the spin moments of nickel ions. The powder sample undergoes a transition into the antiferromagnetic ordered state at  $T_N = 23$  K [4]. In single crystals, the magnetic transitions were observed at temperatures of 28.5 K [8] and 21 K [7]. Magnetization measurements indicate that there is no ferromagnetic moment in the ordered state [7]. The direction of the easy axis was found orthogonal to the  $bc$ -plane. The anisotropic character of the magnetic susceptibility was found in [7, 8] as well. In one aspect, the result in [8] is striking: in the susceptibility measurement taken along the  $b$ -axis, there is no trace of any anomaly related to the magnetic ordering. The latter observation is incompatible with the standard Néel-type ordering pattern and indicates a complex magnetic structure (as well as magnetism in general) of  $\text{Ni}_5(\text{TeO}_3)_4\text{Cl}_2$ .

In high-field electron-spin resonance investigations of  $\text{Ni}_5(\text{TeO}_3)_4\text{Cl}_2$  single crystal, ten spin-resonance modes with characteristic magnetic-field dependences were discovered [6]. Two of them are degenerate in the zero field, and three appear only in high magnetic fields. The two-dimensional model discussed by Mihaly et al. [6] reproduces only a part of the observed excitations, and further investigations including neutron and Raman scattering are necessary for a complete exploration of the magnetic structure in this compound.

Here, we report the first Raman scattering study of a nickel-tellurium-oxychloride  $\text{Ni}_5(\text{TeO}_3)_4\text{Cl}_2$  single crystal in the temperature range above and below  $T_N$ . Raman spectroscopy can probe simultaneously excitations arising from spin and lattice degrees of freedom and, thus, can shed light on the low-temperature magnetic ground state, magnetic anisotropy, and a role of the geometric frustration.

## 2. Experiment

The Raman spectra were measured on an oriented single-crystal sample of dimensions  $3 \times 4 \times 0.2$  mm $^3$  with the

$b$  and  $c$  axis which are parallel to the edges of the slab. The 632.8-nm line of a He–Ne ( $\sim 30$  mW) laser was used in the experiments to reduce the beam-induced heating of the orange colored  $\text{Ni}_5(\text{TeO}_3)_4\text{Cl}_2$  sample, as well as to enhance the scattered light intensity. The scattered light was analyzed with a double Jobin Yvon U1000 monochromator and detected with a cooled photomultiplier RCA 31034 and a photon counting system. The right-angle scattering geometry was used. The laboratory coordinates  $X$  and  $Z$  were chosen to be parallel to the  $c$  and  $b$  axes of the crystal, respectively, while  $Y$  is perpendicular to  $cb$  plane.

The temperature interval of 5–300 K was covered using an optical cryostat. The sample was kept in the exchange gas atmosphere. The sample temperature was monitored by a copper-constantan thermocouple, but taking the local heating of the sample due to the laser irradiation into consideration, the proper temperature was estimated from the Stokes/anti-Stokes intensity ratios.

## 3. Results and Discussion

The crystal  $\text{Ni}_5(\text{TeO}_3)_4\text{Cl}_2$  is monoclinic, of space group  $C2/c$  ( $C_{2h}^6$ ),  $Z = 4$  with the following unit cell dimensions:  $a = 19.5674$  Å,  $b = 5.2457$  Å,  $c = 16.3084$  Å, and  $\beta = 125.29^\circ$  [4]. The primitive unit cell contains two formula units. Since the crystal is inversion-symmetric, the irreducible representations are symmetric ( $g$ ) or antisymmetric ( $u$ ). A normal mode decomposition of the space group gives

$$\Gamma_{vib} = 34A_g + 35B_g + 34A_u + 35B_u.$$

Of the total 138  $\Gamma$ -point phonon modes, 66 are infrared-active, and 69 are Raman-active. According to group theory,  $A_g$  and  $B_g$  modes are allowed for  $XX, YY, ZZ, XY, YX$  and  $XZ, YZ, ZX, ZY$  scattering configurations, respectively [9].

In Fig. 2,*a*, the low-temperature (15 K) polarized Raman spectra of  $\text{Ni}_5(\text{TeO}_3)_4\text{Cl}_2$  in the frequency region of 3–260 cm $^{-1}$  are shown. Narrow and well-distinguished phonon peaks with different intensities are observed. Spectra are well polarized with the leakage of forbidden modes not exceeding 5% intensity of the allowed ones. The above-mentioned characteristics of the system surely allow identifying the number and the symmetry of all phonon modes. Figures 2,*b* and 2,*c* show Raman spectra in the frequency regions 260–550 and 550–900 cm $^{-1}$ , respectively. It is necessary to note that the phonon peaks in Figs. 2,*b* and 2,*c* have a larger

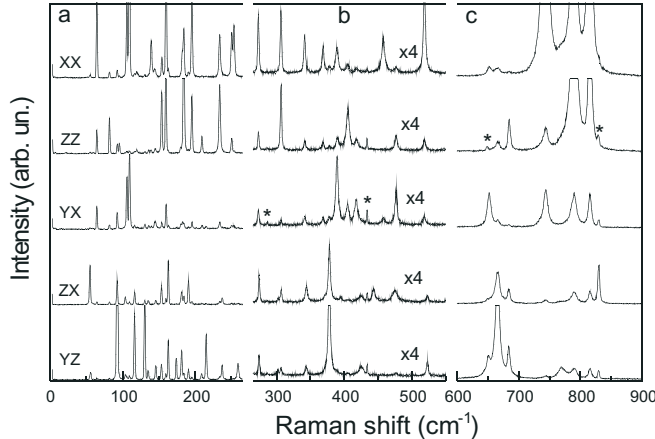


Fig. 2. Raman spectra of the  $\text{Ni}_5(\text{TeO}_3)_4\text{Cl}_2$  single crystal in various scattering configurations ( $T = 15 \text{ K}$ ). Spectral resolution is  $1.8, 1.8$ , and  $3.0 \text{ cm}^{-1}$  in (a), (b), and (c), respectively. The asterisks in all Raman spectra denote laser plasma lines

intensity and linewidth in the higher frequency region. Large differences in the intensities of the Raman tensor components  $XX$ ,  $ZZ$ , and  $YX$  of most  $A_g$  modes are observed. This simply reflects the high optical anisotropy of the material.

Precise measurements allowed us to observe weak and broad Raman spectra at low temperatures in the low-frequency region of  $20\text{--}50 \text{ cm}^{-1}$  (Fig. 3,(a)). These lines are seen in the  $XX$  and  $ZZ$  scattering geometries.

We will focus now on the temperature dependence of the Raman line intensities, frequencies, and linewidths extracted by fitting the corresponding spectra. Three lines with frequencies of  $22.3, 29.4$ , and  $49.0 \text{ cm}^{-1}$  fade away with increasing temperature and are not seen in the spectra at  $T = 25 \text{ K}$  (Fig. 3,(b)), while lines with frequencies  $> 50 \text{ cm}^{-1}$  (except the line at  $55.1 \text{ cm}^{-1}$ , and this frequency region will be discussed later) show no anomalies with temperature and can be identified as phonons. The experimental Raman peak frequencies (in the unit of wave numbers) and the symmetries of all modes are presented in Table 1. Of the 69 phonon modes maximally expected for the monoclinic  $C_{2h}^6$  structure,  $62 (32A_g + 30B_g)$  phonon modes were clearly discovered in Raman experiments.

With decreasing temperature up to  $15 \text{ K}$ , no extra phonon modes appear in Raman spectra, by indicating that  $\text{Ni}_5(\text{TeO}_3)_4\text{Cl}_2$  has no structural transformation in this temperature region.

Following the earlier assignments [10, 11], the modes in the highest-frequency well-separated region of Raman spectra ( $> 650 \text{ cm}^{-1}$ ) can be attributed to the stretching

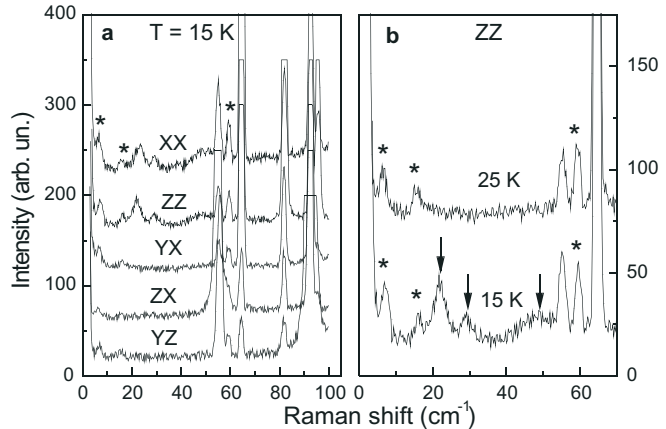


Fig. 3. (a) Low-frequency polarized Raman spectra of  $\text{Ni}_5(\text{TeO}_3)_4\text{Cl}_2$  ( $T = 15 \text{ K}$ ). (b) Raman spectra at  $15$  and  $25 \text{ K}$  (below and above  $T_N$ ) in the  $ZZ$  polarization configuration. The arrows indicate bands which appear in the antiferromagnetic phase. Spectral resolution is  $1.8 \text{ cm}^{-1}$

modes of Te–O bonds. For an isolated  $\text{TeO}_3^{2-}$  group, there are the symmetric and antisymmetric stretchings of the Te–O bonds ( $\nu_1(A_1)$  and  $\nu_3(E)$  with frequencies of  $758$  and  $703 \text{ cm}^{-1}$ , respectively) [10]. In our experiments, we have observed ten ( $5A_g + 5B_g$ ) out of the twelve ( $6A_g + 6B_g$ ) Te–O stretching modes predicted for the monoclinic  $C_{2h}^6$  structure of the crystal  $\text{Ni}_5(\text{TeO}_3)_4\text{Cl}_2$ .

In the frequency region  $250\text{--}550 \text{ cm}^{-1}$ , the symmetric and antisymmetric bending modes of O–Te–O bonds ( $\nu_2(A_1)$  and  $\nu_4(E)$ ) are expected. Ni–O and Ni–Cl bonds vibrations are expected in this frequency region as well [10, 12]. Phonons with energies  $< 250 \text{ cm}^{-1}$  can be attributed as translational and vibration modes [11]. Assignments of vibration modes in the different spectral regions are not strict, since the motion of nickel and fluorine ions is partially coupled with vibration and bending modes of  $\text{TeO}_3^{2-}$  units.

In Fig. 3,*b*, we show the low-frequency part of the Raman spectra of  $\text{Ni}_5(\text{TeO}_3)_4\text{Cl}_2$  at two temperatures, namely above and below  $T_N$  [4, 7]. As clearly seen, three weak and broad lines are observed at  $15 \text{ K}$ . The disappearance of these lines just above  $T_N$  is typical of one-magnon excitations. The one-magnon mode is Raman active by virtue of spin-orbit couplings. The pronounced one-magnon excitations suggest the strong magnetic anisotropy, consistent with electron-spin resonance results [6]. At the same time, the observation of one-magnon excitations only in diagonal components of the Raman tensor is somewhat unusual. A complicate spin lattice might be responsible for that.

Electron-spin resonance investigations [6] revealed that the nature of magnetism in the studied compound is quite complex and cannot be interpreted at present in all details. There are some reasons for such a complexity: (i) nonequivalent crystallographic positions of  $\text{Ni}^{2+}$  ions in distorted octahedral coordinations, (ii) essentially different distances between magnetic ions, which leads to a difference of exchange interactions, and (iii) significant magnetic anisotropy. While the exchange-interaction model used to describe  $\text{Ni}_5(\text{TeO}_3)_4\text{Cl}_2$  [6] correctly explains some properties of the low-energy magnetic excitations, the authors noted the importance of further investigations for the complete description of this compound.

$\text{Ni}_5(\text{TeO}_3)_4\text{Cl}_2$  has a layered structure with  $\text{Ni}_5\text{Te}_4\text{O}_{12}$  sheets and chlorine in the space between sheets. Magnetic  $\text{Ni}^{2+}$  ions have three different crystallographic positions and are located inside of  $\text{NiO}_6$  and  $\text{NiO}_5\text{Cl}$  octahedra. Five Ni-octahedra form a structural unit with a “claw” shape (see Fig. 1). Each

“claw” unit is linked via eight corners to its four nearest neighbors. The magnetic unit cell of  $\text{Ni}_5(\text{TeO}_3)_4\text{Cl}_2$  has twenty  $\text{Ni}^{2+}$  ions (ten  $\text{Ni}^{2+}$  ions on each of the two NiO sheets). Since the coupling between sheets is expected to be weak, it is reasonable to consider the antiferromagnetic structure of  $\text{Ni}_5(\text{TeO}_3)_4\text{Cl}_2$  with ten magnetic sublattices formed by  $\text{Ni}^{2+}$  ions in a single layer.

In Table 2, we present the energies of magnetic excitations from Raman scattering investigations together with the data from [6,7]. The frequencies of magnetic excitations agree with the corresponding modes of resonance investigations [6] (see Table 2). In our Raman experiment, we did not observe two lines with the lowest energies identified earlier as antiferromagnetic resonance modes [7, 13–15]. Perhaps, a low intensity or insufficiently low temperatures of our Raman experiment did not allow us to observe them. We note that antiferromagnetic resonance modes in the isostructural compound  $\text{Ni}_5(\text{TeO}_3)_4\text{Br}_2$  were observed only at temperatures  $T < \frac{1}{2}T_N$  [13–15],

**T a b l e 1.** Frequencies (in  $\text{cm}^{-1}$ ), scattering configurations, and symmetry of the phonon Raman lines in the  $\text{Ni}_5(\text{TeO}_3)_4\text{Cl}_2$  crystal at 15 K. Error in the determination of frequencies is equal to  $\pm 0.2 - \pm 0.4 \text{ cm}^{-1}$  depending on the intensity and width of phonon lines

Frequency ( $\text{cm}^{-1}$ )	Symmetry	Experimental scattering geometry	Frequency ( $\text{cm}^{-1}$ )	Symmetry	Experimental scattering geometry	Free $\text{TeO}_3$ Unit [10] ( $\text{cm}^{-1}$ )
55.1	$B_g$	ZX	253.4	$A_g$	XX	
64.5	$A_g$	XX	259.0	$B_g$	YZ	
81.8	$A_g$	ZZ	272.8	$A_g$	XX	
92.5	$B_g$	YZ	273.8	$B_g$	ZX,YZ	
95.4	$A_g$	ZZ	301.8	$B_g$	ZX	
103.8	$B_g$	ZX	306.3	$A_g$	ZZ,XX	$\nu_4(E)$
105.8	$A_g$	ZZ,XX	341.5	$A_g$	XX	326
109.4	$A_g$	XX,YX	343.8	$B_g$	YZ	
116.5	$B_g$	YZ	368.5	$A_g$	XX	
119.6	$A_g$	XX	377.9	$B_g$	YZ	
130.5	$B_g$	YZ	389.3	$A_g$	XX,YX	$\nu_2(A_1)$
134.8	$B_g$	YZ	395.0	$B_g$	ZX	364
139.2	$A_g$	XX	405.0	$A_g$	ZZ	
144.5	$A_g$	XX,YX	417.9	$A_g$	YX	
145.6	$B_g$	YZ	425.0	$B_g$	ZX,YZ	
153.5	$B_g$	ZX,YZ	443.7	$B_g$	ZX	
153.8	$A_g$	ZZ	457.9	$A_g$	XX	
159.7	$A_g$	ZZ,XX	474.6	$B_g$	ZX	
162.9	$B_g$	ZX,YZ	476.8	$A_g$	YX	
174.0	$B_g$	YZ	518.8	$A_g$	XX	
181.4	$B_g$	YZ	523.2	$B_g$	YZ	
182.5	$A_g$	XX	651.1	$B_g$	YZ	
184.4	$A_g$	ZZ	652.3	$A_g$	YX	
190.7	$B_g$	ZX	666.0	$B_g$	YZ	
195.4	$A_g$	ZZ,XX	684.2	$B_g$	YZ	$\nu_3(E)$
209.0	$B_g$	YZ	684.9	$A_g$	ZZ	703
209.4	$A_g$	ZZ	743.9	$A_g$	XX	
215.1	$B_g$	YZ	770.1	$B_g$	YZ	
233.7	$A_g$	ZZ	789.9	$A_g$	ZZ,XX	$\nu_1(A_1)$
237.1	$B_g$	YZ	815.6	$A_g$	ZZ,XX	758
250.3	$A_g$	XX	829.9	$B_g$	ZX	

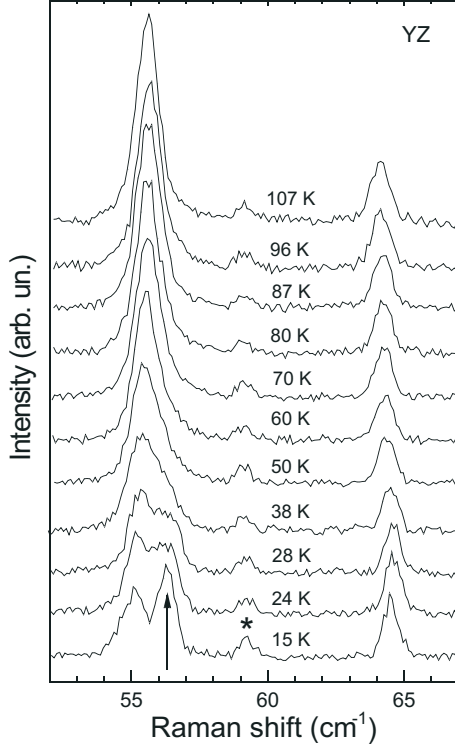


Fig. 4. Temperature dependent Raman spectra in the frequency region  $52\text{--}67\text{ cm}^{-1}$  in the  $YZ$  polarization. Spectral resolution is  $0.6\text{ cm}^{-1}$ . The arrow indicates a Raman line with unexpected temperature behavior

and that is why strong spin fluctuations were suggested in the temperature region  $\frac{1}{2}T_N < T < T_N$ .

A wide band at  $\sim 49\text{ cm}^{-1}$  came into the frequency region of a twofold degenerate mode at  $46\text{ cm}^{-1}$  [6] which splits into two modes only in finite magnetic fields. Perhaps, this wide band splits in the Raman experiment at lower temperatures or in a magnetic field.

**T a b l e 2.** Comparison of Raman data (at  $15\text{ K}$ ) with frequencies of spin resonance modes (at  $2.5\text{ K}$ ) [6]. Asterisks denote the modes which are visible only at high fields, and their zero-field frequencies were determined in [6] by extrapolation from a finite field to zero

Raman data at $T = 15\text{ K}$	[6] at $T = 2.5\text{ K}$	[7]
	13.5	11.0
	17.3	13.2
$22.3 \pm 0.5$ (XX, ZZ)	24.4	
	25.5*	
$29.4 \pm 0.5$ (XX, ZZ)	29*	
	32.2	
$49.0 \pm 1.0$ (XX, ZZ)	46 (2)	
$56.3 \pm 0.1$ (YZ)	56	
	63*	
	68.5 (2)	

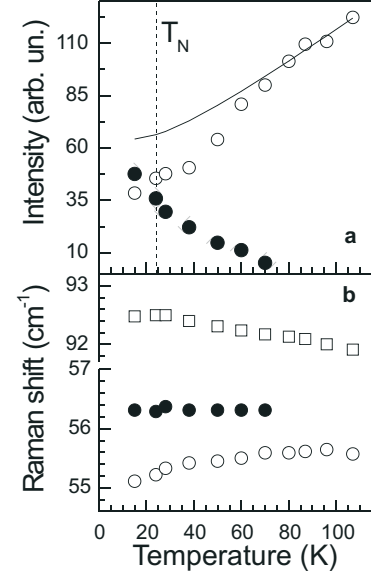


Fig. 5. Plot of the integrated intensities of the lines at around  $55$  and  $56\text{ cm}^{-1}$  (a) and peak positions of the respective line and a phonon line at  $92.5\text{ cm}^{-1}$  versus temperature (b). The solid curve shows the expected temperature dependence for a harmonic oscillator with a frequency of  $55.1\text{ cm}^{-1}$

At last, we will turn to the discussion of an intriguing feature with unexpected temperature behavior which is present in the Raman spectra at low temperatures (Fig. 4). The frequency of the  $56.3\text{-cm}^{-1}$  mode observed at  $T = 15\text{ K}$  in the Raman spectra coincides with that of a spin-resonance mode at  $56\text{ cm}^{-1}$  [6]. Its peak position is practically temperature independent. The notable thing is that this line vanishes around  $70\text{ K}$  ( $\approx 2.8T_N$ ), well above  $T_N$ . A remarkable observation is that the  $56.3\text{-cm}^{-1}$  mode is coupled with the  $55.1\text{-cm}^{-1}$   $B_g$  phonon mode. As clearly seen from Fig. 5, the  $55.1\text{-cm}^{-1}$  mode softens nonlinearly with decreasing temperature in contrast with all other phonon modes. Also the  $55.1\text{-}$  and  $56.3\text{-cm}^{-1}$  modes show different behaviors in their intensities (see Figs. 4 and 5). The  $56.3\text{-cm}^{-1}$  mode increases in intensity with decreasing temperature, while the  $55.1\text{-cm}^{-1}$  mode decreases in intensity for temperatures below  $T \approx 70\text{ K}$  with deviations from the expected Bose-Einstein behavior.

The nature of the  $56.3\text{-cm}^{-1}$  magnetic mode is not clear. An interpretation in terms of one-magnon excitations does not agree with its temperature behavior, namely its persistence to temperatures far above  $T_N$ . On the other hand, the interpretation of this mode as two-magnon excitations is unconvincing due to its linewidth which is narrow and comparable to the linewidth

of phonon modes. Moreover, it was shown that the frequency position of the  $56\text{-cm}^{-1}$  mode has a strong dependence on an applied magnetic field [6], which is not characteristic of two-magnon excitations [16]. The above-presented arguments allow us to speculate that this peak is related to a crystal field excitation of  $\text{Ni}^{2+}$  ions in the  $[\text{Ni}_5\text{O}_{17}\text{X}_2]$  "claw" unit in the paramagnetic state. The degenerated ground state  $^3\text{F}$  of the free ion  $\text{Ni}^{2+}$  splits into discrete levels under the combined effect of the spin-orbit and crystal field interactions, and the electronic transitions between split levels of the ground state are allowed in the Raman scattering. In  $\text{Ni}_5(\text{TeO}_3)_4\text{Cl}_2$ , the crystal field splitting scheme can be different for different  $\text{Ni}^{2+}$  ions, depending strongly on the crystallographic ion coordination and the crystal field strength.

We hope that our further investigations, namely the Raman scattering studies at lower temperatures and in an applied magnetic field, will help one to clear up some of the very interesting features of the peculiar compound  $\text{Ni}_5(\text{TeO}_3)_4\text{Cl}_2$  which are still under debates.

#### 4. Conclusions

The Raman spectra of a single crystal  $\text{Ni}_5(\text{TeO}_3)_4\text{Cl}_2$  have been measured and analyzed. In different scattering geometries, we observed 62 phonon modes out of the 69 ones predicted by a group-theoretic analysis for the monoclinic  $C_{2h}^6$  lattice symmetry. The temperature behavior of the phonon modes testifies to the absence of a structural phase transition in the temperature range 15–300 K. At low temperatures, a number of additional weak peaks appear in the low-energy Raman spectra. Three of them with frequencies of 22.3, 29.4, and  $49.0\text{ cm}^{-1}$  vanish at around  $T_N$  with rising temperature. This is a typical behavior for the one-magnon scattering. The line at  $56.3\text{ cm}^{-1}$  exhibits the anomalous temperature dependence; with increasing temperature, it disappears at around  $2.8 T_N$ . Moreover, this line displays a strong interaction with the phonon mode at  $55.1\text{ cm}^{-1}$ . Further, Raman investigations will be carried out to complete the exploration of the  $\text{Ni}_5(\text{TeO}_3)_4\text{Cl}_2$  compound.

V. Gnezdilov thanks the Ukrainian-Russian grant N 8-2008 for the support.

1. P. Lemmens, G. Güntherodt, and C. Gros, Phys. Rep. **376**, 1 (2003) and references therein.
2. D.A. Tennant, *et al.*, Phys. Rev. **67**, 054414, (2003).
3. F. Mila, Eur. J. Phys. **21**, 499 (2000).

4. M. Johnsson, K.W. Tornroos, P. Lemmens, and P. Millet, Chem. Mater. **15**, 68 (2003).
5. M. Pregelj, A. Zorko, H. Berger, H. van Tol, L.C. Brunel, A. Ozarowski, S. Nellutla, Z. Jaglicic, O. Zaharko, P. Tregenna-Piggott, and D. Arcon, Phys. Rev. B **76**, 144408 (2007).
6. L. Mihaly, T. Feher, B. Dora, B. Nafradi, H. Berger, and L. Forro, Phys. Rev. B **74**, 174403 (2006).
7. S.L. Gnatchenko, M.I. Kobets, E.N. Khatsko, M. Baran, R. Szymczak, P. Lemmens, and H. Berger, Low Temp. Phys. **34**, in press (2008).
8. R. Becker, M. Prester, H. Berger, M. Johnsson, D. Drobac, and I. Zivkovic, Sol. State Sci. **9**, 223 (2007).
9. H. Poulet, J.-P. Mathieu, *Spectres de Vibration et Symetrie des Cristaux* (Gordon and Breach, Paris, 1970).
10. K. Nakamoto, *Infrared and Raman Spectra of Inorganic and Coordination Compounds* (Wiley-Interscience, New York, 1986).
11. L. D'Alessio, F. Pietrucci, and M. Bernasconi, J. Phys. Chem. Solids **68**, 438 (2007).
12. Yu.G. Pashkevich, V.A. Blinkin, V.P. Gnezdilov, V.V. Tsapenko, V.V. Eremenko, P. Lemmens, M. Fischer, M. Grove, G. Güntherodt, L. Degiorgi, P. Wachter, J.M. Tranquada, and D.J. Buttrey, Phys. Rev. Lett. **84**, 3919 (2000).
13. D. Arcon, A. Zorko, M. Pregelj, J. Dolinsek, H. Berger, A. Ozarowski, H. van Toll, and L.C. Brunel, J. Magn. Magn. Mater. **316**, e349 (2007).
14. A. Zorko, D. Arcon, J. Dolinsek, Z. Jaglicic, A. Jeromen, H. van Tol, and H. Berger, J. Phys.: Condens. Matter **19**, 145278 (2007).
15. M. Pregelj, D. Arcon, A. Zorko, O. Zaharko, L.C. Brunel, H. van Tol, L.C. Brunel, A. Ozarowski, S. Nellutla, and H. Berger, Physica B **403**, 950 (2008).
16. M. Cottam and D. Lockwood, *Light Scattering in Magnetic Solids* (Wiley, New York, 1986).

РАМАНОВЕ РОЗСІЯННЯ СВІТЛА В ДВОВИМІРНІЙ  
 $S = 1$  КВАНТОВІЙ СПІНОВІЙ СИСТЕМІ  $\text{Ni}_5(\text{TeO}_3)_4\text{Cl}_2$

О.В. Песчанський, В.П. Гнєзділов, В.І. Фомін,  
 В.В. Єременко, П. Лемменс, К.-Й. Чої, Х. Бергер

Р е з ю м е

Телуровий оксохлорид перехідного металу,  $\text{Ni}_5(\text{TeO}_3)_4\text{Cl}_2$ , було досліджено методом спектроскопії рamanового розсіяння світла в інтервалі температур 15–300 K. Шістдесят дві фононні моди (із загальною кількості 69 раман-активних фононних мод, що дозволені для моноклинної  $C_{2h}^6$ -структур) були ідентифіковані в спектрах та їх поведінка проаналізована. Декілька додаткових особливостей було виявлено при низьких температурах: а) три низькочастотні полоси ( $22.3, 29.4$  и  $49.0\text{ cm}^{-1}$  при  $T = 15\text{ K}$ ) з температурною поведінкою, що характерна для одномагніонного розсіяння, та б) полоса з частотою  $56.3\text{ cm}^{-1}$  та незвичайною температурною поведінкою. Обговорена можлива природа низькотемпературних полос в рamanових спектрах.